

# Solid to Quasi-Liquid Phase Transition of Submonolayer Pentacene

Received 2 May, 2023; revised 29 June, 2023; accepted 13 July, 2023

Eunji Sim<sup>a,b,c</sup>, Mihyun Yang<sup>d</sup>, Ha Eun Cho<sup>a,e</sup>, Somang Koo<sup>a</sup>, Seong Chu Lim<sup>b,c,\*</sup>, and Kyuwook Ihm<sup>a,\*</sup>

<sup>a</sup>Beamline Research Division, Pohang Accelerator Laboratory, Pohang 37673, Republic of Korea

<sup>b</sup>Department of Energy Science, Sungkyunkwan University, Suwon 16419, Republic of Korea

<sup>c</sup>Department of Smart Fabrication Technology, Sungkyunkwan University, Suwon 16419, Republic of Korea

<sup>d</sup>Surface Property Analysis Team, LG Display, Paju 10845, Republic of Korea

<sup>e</sup>Department of Physics, University of Ulsan, Ulsan 44610, Republic of Korea

\*Corresponding author E-mail: seonglim@skku.edu, johnet97@postech.ac.kr

## ABSTRACT

Based on surface charge states, the thermodynamics of pentacene molecules exhibit intriguing structural transitions with various temperatures. On an SiO<sub>2</sub> surface, the mean tilt angle decreases with increasing temperature, whereas three different structural regimes form on the Au surface. To understand these contrasting temperature dependencies of molecular orientation on the two surfaces, a model wherein the tilt angle  $\alpha$  has two stable states is proposed in this study. Consequently, the pentacene crystals undergoes a phase transition at a relatively low temperature of 350 K, thus indicating a hidden factor governing the morphology of molecular crystals, and providing insights into the thermal behavior of physisorbed organic molecules.

**Keywords:** Surface melting, Phase transition, Organic crystal, Pentacene

## 1. Introduction

Physically adsorbed organic films have attracted considerable attention owing to their potential applications as inhibitor layers for area-selective deposition (ASD) [1–5] and electronic devices [6,7]. Intermolecular and molecule-substrate interactions are crucial in determining the degree of crystallinity of organic films, which is directly related to the area selectivity in ASD or charge mobility in electronic devices [8,9]. However, because these phenomena are based on weak van der Waals interactions, the crystallinity of molecular film formed on the surface is affected by small external stimuli and sensitive changes. Particularly, the surface charge density is a sensitive determinant of the crystallinity of a molecular film, and its understanding is crucial for improving the selectivity of area-selective film formation.

Pentacene is a model system for organic crystal films based on van der Waals interactions. Depending on their substrate, pentacene molecular films exhibit dramatic variations in their structural ordering. The charge-carrier mobility is directly dependent on the crystallinity of the grown organic film, whose reported value is in the range of 0.1–58.0 cm<sup>2</sup>V<sup>-1</sup>s<sup>-1</sup> [10]. Studies on the structural ordering of pentacene films under various conditions have demonstrated that the initial arrangement of pentacene molecules on the surface acts as a nucleation seed. [11–13]. On the crystal structure surface, the pentacene molecule exhibits two orientations, i.e., standing-up or lying-down, which are observed when the angle  $\alpha$  between the longitudinal axis of pentacene molecule and surface is greater than 70° or less than 10°, respectively [3].

In the early stage of pentacene growth, the standing-up orientation is important for obtaining highly ordered crystalline structures, owing to the lower surface energy of (001) crystal plane compared with that of the other planes [14,15]. Therefore, the growth directions of (122),

(011), and (121) planes can be varied to (001) [13].

On the substrate, pentacene molecules interact with surface electrons and neighboring molecules with energies of  $E_{ms}$  and  $E_{mm}$ , respectively.

At a given temperature during the early stage of crystallization, the energy difference between  $E_{ms}$  and  $E_{mm}$  is crucial in determining the orientation  $\alpha$  of the pentacene molecules [3,12,16]. However, as the substrate temperature increases, the variation in average orientation ( $\alpha$ ) is independent of the type of growth substrate [7,13,17].

In this study, the near-edge X-ray absorption fine structure (NEXAFS) spectroscopy was used to analyze the temperature dependence of low-coverage pentacene molecules on silicon dioxide (SiO<sub>2</sub>) and gold (Au) surfaces. To explain the observed variations in  $\alpha$ , a thermodynamic model was developed for the two orientations (standing-up and lying-down) of pentacene. Using this model, the intermolecular interactions were abruptly weakened and induced by a phase transition of the pentacene crystal from solid to quasi-liquid at 350 K.

## 2. Experimental details

The sample preparation and spectroscopic measurements were performed at the 4D NEXAFS beamline of the Pohang Accelerator Laboratory. Si with a thermal oxide layer (100 nm) and polycrystalline Au of dimensions 5 × 10 cm<sup>2</sup> were simultaneously mounted on a grounded molybdenum holder, which was thermally linked to a resistive heater wrapped in phosphor-boron-nitride. For degassing, the substrates were annealed in an ultrahigh vacuum chamber (base pressure: 4 × 10<sup>-10</sup> Torr) at 670 K for 48 h. Prior to sample heating, surface contaminants were cleaned using ion sputtering for 10 min (Ar<sup>+</sup>, 3 KeV), and the cleanliness of the substrate surfaces was confirmed by using X-ray photoemission spectroscopy (XPS).



Pentacene (Aldrich, purified by gradient sublimation) was thermally evaporated onto the SiO<sub>2</sub> and Au surfaces at room temperature (RT) and deposition rate of 0.05 Ås<sup>-1</sup>. The deposition rate and thickness of the pentacene layer were monitored using a crystal-oscillator thickness monitor (Inficon XTC). The temperature of the sample was regulated within ±0.1 K. The partial electron yield (PEY)-mode NEX-AFS was measured by counting the carbon KLL Auger electrons.

### 3. Results and discussion

The temperature-dependent desorption patterns of 100 nm pentacene films grown on SiO<sub>2</sub> and Au were observed using optical microscopy. As the temperature increased, the inhomogeneous and homogenous desorption of pentacene film was observed on SiO<sub>2</sub> and Au surfaces, respectively (Fig. 1). In the former case, the desorption was initiated by the defect sites denoted by the red arrows in Fig. 1b, which continued to evolve gradually around the defect centers [Figs. 1(c) and 1(d)]. Therefore, the intermolecular interaction energy ( $E_{mm}$ ) or cohesive energy of neighboring molecules in the film is greater than the molecule-substrate interaction energy ( $E_{ms}$ ). Because the molecules at the defect site are outside their normal positions, their binding energies with neighboring molecules is considerably weakened. In the absence of pentacene, the molecules were desorbed on the substrate; hence, the interaction energy  $E_{mm}^D$  between the molecules at the defect site can be described as  $E_{ms} < E_{mm}^D < E_{mm}$  [14,15]. If the thermal energy falls within the range of  $E_{mm}^D - E_{mm}$ , desorption initiates from the defect center owing to the unrestricted mobility of molecules at the defective site, which are detached from the substrate and neighboring molecules. Consequently, the desorption process exhibits inhomogeneity, similar to the observed behavior of pentacene on SiO<sub>2</sub>.

Compared with the SiO<sub>2</sub> surface, the Au surface contains a larger number of crystal defects; hence, the pentacene molecules exhibit homogeneous desorption from the Au surface [13]. This can be attributed to the interaction energies of pentacene molecules formed on Au, which are in the order  $E_{mm}^D < E_{mm} < E_{ms}$ . Herein, desorption occurred when the thermal energy of molecule was greater than its binding energy with the substrate, thus implying that thermal desorption cannot discern the intermolecular interaction energy at the defective sites [Figs. 1(e) and 1(f)].

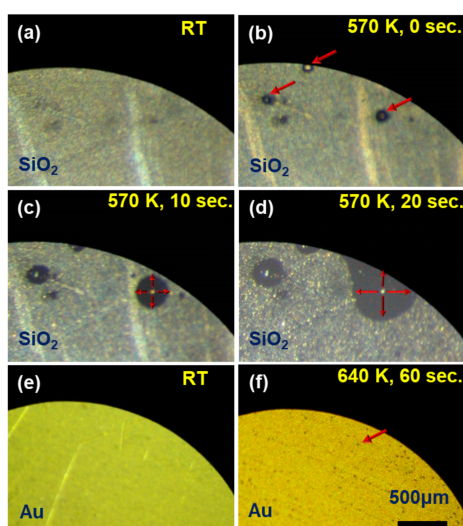


**Figure 1.** Optical images of inhomogeneous desorption of pentacene molecules on SiO<sub>2</sub> surface. Pentacene thin film (100 Å) on SiO<sub>2</sub> surface at: (a) room temperature (RT), (b)–(d) after annealing at 570 K for (b) 0 s, (c) 10 s, and (d) 20 s. Homogeneous desorption of pentacene molecules on Au surface. Pentacene thin film (100 Å) on Au at: (e) room temperature, and (f) 640 K after complete desorption of molecules for 60 s.

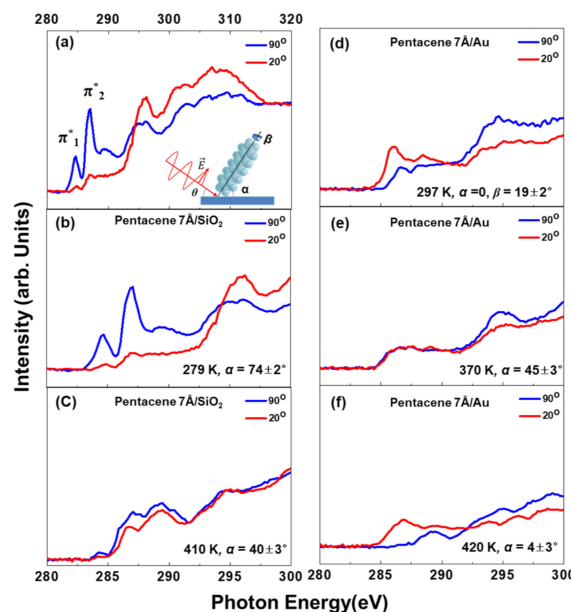


**Figure 2.** (a) NEXAFS spectra of a pentacene molecules (7 Å) grown on an SiO<sub>2</sub> surface at photon incident angles of 20° (red line) and 90° (blue line). The inset of (a) shows experimental geometry of polarization-dependent NEXAFS spectroscopy with photon incident angle  $\theta$ , when the molecule has tilt angles  $\alpha$  and  $\beta$  with the surface. Enlarged NEXAFS spectrum in the 280–300 eV region of pentacene on SiO<sub>2</sub> surface at: (b) RT and (c) 410 K. (d)–(f) NEXAFS spectra of pentacene (7 Å) on the Au surface at: (d) RT, (e) 370 K, and (f) 420 K; here, the photon incident angles are 20° (red line) and 90° (blue line).

To analyze the molecular orientation of sub-monolayer, a 7 Å-thick layer (approximately 0.5 molecular layers) of pentacene molecules was simultaneously deposited on cleaned SiO<sub>2</sub> and Au. Furthermore, NEX-AFS measurements were performed in vacuum [14,15].

The NEXAFS spectra of an as-prepared sample were recorded at incident angles  $\theta_i$  of 20° (red) and 90° (blue) [Figs. 2(a) and 2(d)] [18, 19]. The overall line shape of the NEXAFS spectra of pentacene on the substrates is similar to that of gas-phase pentacene, thus indicating that pentacene molecules do not chemically bond with SiO<sub>2</sub> on the Au surface [20]. In the Fig. 2(a), the peaks  $\pi_1^*$  and  $\pi_2^*$  at 284.7 and 287 eV, respectively, are attributed to the resonant electrons generated during the relaxation process of excited electron from C 1s to  $\pi^*$  antibonding orbital. Furthermore, the broad features above 290 eV originate from  $\sigma^*$  resonances [16].

Because the  $\pi^*$  orbital is strongly localized perpendicular to the plane of the carbon ring of pentacene molecule, the  $\pi^*$  resonance peak strongly depends on the polarization of electric field. Therefore, the angle-dependent NEXAFS spectra can be used to probe the orientation of pentacene molecules [Fig. 2(a)].

The peak intensity  $I_{\pi^*}$  depends on the molecular tilt angle ( $\alpha$ ) and photon incident angle  $\theta$  as  $I_{\pi^*} = P/3 [1 + (3 \cos^2 \theta - 1)(3 \cos^2(\pi/2 - \alpha) - 1)/2]$ , where  $P$  is the polarization ratio of the incident photon and  $\beta$  is the azimuthal rotation about the longitudinal axis of molecule [Fig. 2(a)] [21]. The  $p$ -value of the used beamline was 0.8 [Fig. 2(a)].

To evaluate the average ( $\alpha$ ) values at each temperature, the NEX-AFS spectra at  $\theta_i = 20, 45, 70,$  and  $90^\circ$  of photon incidence were acquired. At RT, pentacene on SiO<sub>2</sub> surface exhibited strong angular dichroism of the  $\pi^*$  peak at 287 eV [Fig. 2(b)]. Based on the relationship  $I_{\pi^*}(\theta, \alpha)$ , ( $\alpha$ ) of pentacene molecule on SiO<sub>2</sub> surface at RT was estimated to be 72°, which is close to the tilt angle of crystal phase on SiO<sub>2</sub> in the stand-up orientation [16]. As the temperature increased to above 410 K, the strong dichroic response nearly disappeared [Fig. 2(c)], thus implying that the initial molecular ordering vanishes. This agrees with previous reports on the broadening of X-ray diffraction

patterns of pentacene films grown at elevated temperatures [17,22].

Figures 2(d)-(f) show three different dichroic responses observed on the Au surface. Compared with the pentacene molecule on Si surface, the  $\pi_1^*$  transition peak located at 284.7 eV disappeared for the Au surface [Fig. 2(d)]. This occurs because of the spatial distribution of the  $\pi_1^*$  orbital of pentacene, which predominantly surrounds the outer carbon atoms of the molecule, thus leading to its direct interaction with the valence electrons of the surface Au atoms. As the  $\pi_1^*$  orbital interacts with Au, the electron orbital of pentacene molecule localizes, thereby exhibiting an electronic structure similar to that of poly(*p*-phenylene) [23–25].

At RT, the intensity of  $\pi_2^*$  peak observed at  $\theta_i = 20^\circ$  was greater than that at  $\theta_i = 90^\circ$  [Fig. 2(d)], thus corresponding to average  $\langle \alpha \rangle 19 \pm 2^\circ$  for the angle induced by  $\beta$  and indicating the formation of an adlayer. Pentacene molecules in the first monolayer lie flat ( $\alpha \approx \beta \approx 0^\circ$ ) on the Au surface, whereas those in the adlayer are slightly rotated ( $\alpha \approx 0^\circ$  and  $\beta \approx 20^\circ$ ) [13]. As the temperature of the substrate increased, the tilt angle of the adlayer approached  $45^\circ$  [Fig. 2(e)], which is confirmed by the previous NEXAFS results [13]. When the temperature is increased to 420 K, the  $\pi_2^*$  peak at  $\theta_i = 20^\circ$  is greater than the intensity measured at  $\theta_i = 90^\circ$ , indicating the decrement in molecular tilt angle (estimated  $\langle \alpha \rangle = 89 \pm 3^\circ$ ) [Fig. 2(f)].

To describe the thermodynamic behavior of  $\langle \alpha \rangle$  pentacene molecules on SiO<sub>2</sub> and Au surfaces, a model with the following two stable states of  $\alpha$  was considered: standing-up ( $\alpha = 74^\circ$ ) with  $E = E_{st}$  and lying-down ( $\alpha = 0^\circ$ ) with  $E = E_{ly}$  (Fig. 3) [12]. The energies of surface molecules in these two geometries can be described as  $E_{st} = E_0 - E_{mm} - E_1 + fk_B T/2$  and  $E_{ly} = E_0 - E_{ms} - E_2 + fk_B T/2$ , respectively, where  $E_0$  is the energy of molecule in the gas phase. For molecules in the standing-up geometry,  $E_{mm}$  and  $E_1$  are the interaction energies with the neighboring molecules and surface atoms, respectively;  $E_{ms}$  and  $E_2$  are the interaction energies with the substrate and two molecules in the lying-down orientation, respectively;  $f$  is the degree of freedom of surface pentacene molecule;  $k_B$  is the Boltzmann constant; and  $T$  is the absolute temperature. Because  $E_1$  and  $E_2$  are infinitesimally less than  $E_{mm}$  and  $E_{ms}$  [12,14,15], they are neglected. In this model, the partition function can be written as follows.

$$Z = e^{-\left(\frac{E_0}{k_B T} + \frac{f}{2}\right)} \left[ e^{\frac{E_{ms}}{k_B T}} + e^{\frac{E_{mm}}{k_B T}} \right]. \quad (1)$$

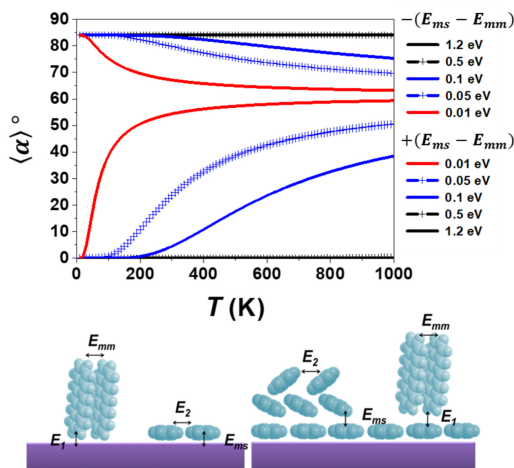


**Figure 3.** Thermodynamic behavior of average tilt angles  $\langle \alpha \rangle$  for various values of  $E_{ms} - E_{mm}$ .  $E_{ms} - E_{mm} < 0$ : pentacene molecules on SiO<sub>2</sub> surface;  $E_{ms} - E_{mm} > 0$ : pentacene molecules on Au surface. Illustration of possible intermolecular interactions  $E_{mm}$  and molecule-substrate interaction  $E_{ms}$ .

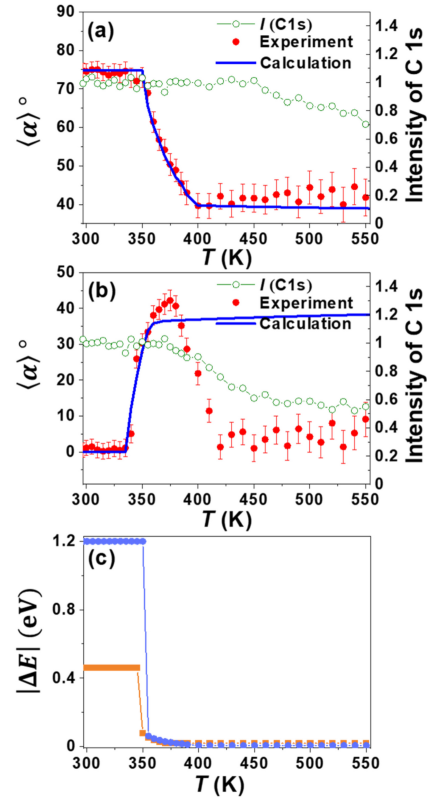


**Figure 4.** Tilt angles acquired from the polarization-dependent partial electron yield (PEY)-NEXAFS spectra of a 7 Å-thick pentacene layer on (a) SiO<sub>2</sub> (circles) and (b) Au (squares) surfaces as a function of temperature; blue line: best fit of calculated curves  $\langle \alpha \rangle$  of pentacene molecules on SiO<sub>2</sub> and Au surfaces with parameters of  $\alpha_{st} = 74^\circ$  and  $\alpha_{ly} = 0^\circ$ , respectively. (c)  $\Delta E$  values used to obtain the best fitted curves represented by blue lines in (a) and (b).

Thereafter, the averaged tilt angle of  $\langle \alpha \rangle$  can be obtained as

$$\langle \alpha \rangle = \frac{1}{Z} \sum_i \alpha_i e^{-\frac{E_i}{k_B T}} = \frac{\alpha_{ly} e^{\frac{\Delta E}{k_B T}} + \alpha_{st}}{e^{\frac{\Delta E}{k_B T}} + 1}, \quad (2)$$

where  $\Delta E = E_{ms} - E_{mm}$ . The curves were calculated for several selected values of  $\Delta E$  (Fig. 3). Herein, two molecular geometries  $\alpha_{st} = 74^\circ$  and  $\alpha_{ly} = 0^\circ$  were used for the two orientations of pentacene molecules. At sufficiently low system temperature, i.e.,  $k_B T \ll |\Delta E|$ , if  $\Delta E < 0$  similar to pentacene on SiO<sub>2</sub> surface,  $\langle \alpha \rangle$  exhibits a standing-up geometry. Contrastingly, if  $\Delta E > 0$  as on the Au surface,  $\langle \alpha \rangle$  exhibits a lying-down geometry in the low energy regime (Fig. 3). When the temperature of the system increases such that  $k_B T \gg |\Delta E|$ ,  $\langle \alpha \rangle$  for the two substrates approaches  $37^\circ$ , thus corresponding to  $(\alpha_{st} + \alpha_{ly})/2$ . Therefore, for sufficiently low or high temperature limits, the model describes the thermal behavior of  $\langle \alpha \rangle$  on the insulating and metal surfaces, as observed using NEXAFS spectroscopy (Fig. 2) [13,17].

Detailed thermal behavior of  $\langle \alpha \rangle$  were acquired using the angular dichroism of the NEXAFS spectra of pentacene molecules at 7 Å on the SiO<sub>2</sub> and Au surfaces [Figs. 4(a) and 4(b)].

The experimental results differed significantly from the smooth transitions predicted by calculations (Fig. 3), thus indicating the absence of an unknown geometric state of  $\alpha$  because the addition of new states in the calculation does not cause the abrupt transition observed in the experimental results. However, the abrupt variation in  $\Delta E$  at a specific temperature explains the experimental results well.

The best fit of the temperature behavior of  $\langle \alpha \rangle$  for the two substrates is indicated by the solid blue lines [Figs. 4(a) and 4(b)]. Notably, the

$\Delta E$  values used for this process decreased sharply to zero at approximately 350 K. Because the  $\Delta E$  value represents the energy difference between the two possible geometries of pentacene molecules on each substrate, the removed energy difference, i.e.,  $\Delta E \approx 0$  eV, indicates that molecular melting occurs near 350 K. Furthermore,  $\Delta E$  of pentacene molecules on the SiO<sub>2</sub> surface was  $\approx 1.2$  eV, which commensurates with the previously reported value of 1.0 eV [12,14,15].

On the Au surface, excluding the contribution of  $\beta$  near RT,  $\langle \alpha \rangle$  was estimated to be approximately 0° [Fig. 4(b)] [13]. As the temperature increased,  $\langle \alpha \rangle$  increased until 380 K and sharply decreased to approximately zero [Fig. 4(b)] owing to the desorption of pentacene adlayer molecules, which is consistent with the findings of a previous report [26]. Above 380 K, the carbon 1s intensity decreased, thus facilitating the desorption of molecule.

After the desorption of adlayer molecules, the NEXAFS spectrum revealed the information regarding the direct binding of pentacene molecules to the Au surface. The desorption of a molecule from the adlayer exposes a flat-lying molecule in the Au monolayer with  $\beta = 0$ . The binding energy of a pentacene molecule bonded directly to the Au surface is 1.82 eV, and such molecules exhibit no desorption in the temperature range of this experiment [26]. Similar to the SiO<sub>2</sub> surface, the fitted curve was derived by adjusting the value of  $\Delta E$  [Figs. 4(b) and 4(c)], thereby revealing information about the pentacene molecules in the adlayer formed on Au substrate, which melted near 350 K.

#### 4. Conclusions

This study investigated the thermal behaviors of pentacene molecules on SiO<sub>2</sub> and Au surfaces using soft X-ray absorption spectroscopy. The initial configuration of these molecules can be explained using two main interactions: intermolecular and molecular-surface. Because the SiO<sub>2</sub> and Au surfaces have significant variations in valence electron densities, they exhibit opposite initial molecular arrangements. Furthermore, a model with two energy states was proposed to adequately describe the thermodynamic behavior of pentacene molecules on the two surfaces by considering an additional phase transition. These results describe the morphologies of pentacene observed at various temperatures. The energy difference  $\Delta E$  between the two geometries of pentacene molecules was removed at 350 K, thus implying the occurrence of a phase transition from solid to quasi-liquid. These findings provide deeper insights into the initial molecular arrangement on surfaces and provide a strategy for growing high-quality molecular crystals based on the surface charge states.

#### Acknowledgments

This study was supported by the National Research Foundation of Korea (NRF) (Grant No. NRF-2018R1D1A1B07043155) from the Ministry of Science, ICT, and Future Planning, Korea. The experiments at the 4D beamline of the PLS-II were supported by MSIP, R. O., Korea.

#### Conflicts of Interest

The authors declare no conflicts of interest.

#### ORCID

Eunji Sim <https://orcid.org/0000-0003-3322-6674>  
Kyuwook Ihm <https://orcid.org/0000-0003-0075-5772>

#### References

- [1] N. E. Richey, C. Paula, and S. F. Bent, *J. Chem. Phys.* 152, 040902 (2020).
- [2] Y. S. Yang, C. Beekman, W. Siemons, C. M. Schlepütz, N. Senabulya, R. Clarke, and H. M. Christen, *APL Mater.* 4, 036106 (2016).
- [3] G. E. Thayer, J. T. Sadowski, F. M. Heringdorf, T. Sakurai, and R. M. Tromp, *Phys. Rev. Lett.* 95, 256106 (2005).
- [4] L. Miozzo, A. Yassar, and G. Horowitz, *J. Mater. Chem.* 20, 2513 (2010).
- [5] A. Cabrero-Vilatela, J. A. Alexander-Webber, A. A. Sagade, A. I. Aria, P. Braeuniger-Weimer, M. -B. Martin, R. S. Weatherup, and S. Hoffman, *Nanotechnology* 28, 485201 (2017).
- [6] M. Halik *et al.*, *Nature* 431, 963 (2004).
- [7] J. Wu, M. Agrawal, H. A. Becerril, Z. Bao, Z. Liu, Y. Chen, and P. Peumans, *ACS Nano* 4, 43 (2010).
- [8] C. A. Schoenbaum, D. K. Schwartz, and J. W. Medlin, *Acc. Chem. Res.* 47, 1438 (2014).
- [9] H.-L. Cheong, Y.-S. Mai, W.-Y. Chou, L.-R. Chang, and X.-W. Liang, *Adv. Funct. Mater.* 17, 3639 (2007).
- [10] O. D. Jurchescu, J. Baas, and T. T. M. Palstra, *App. Phys. Lett.* 84, 3061 (2004).
- [11] R. Lassnig, M. Hollerer, B. Striedinger, A. Fian, B. Stadlober, and A. Winkler, *Org. Electron.* 26, 420 (2015).
- [12] D. Choudhary, P. Clancy, R. Shetty, and F. Escobedo, *Adv. Funct. Mater.* 16, 1768 (2006).
- [13] D. Käfer, L. Ruppel, and G. Witte, *Phys. Rev. B* 75, 085309 (2007).
- [14] J. E. Northrup, M. L. Tiago, and S. G. Louie, *Phys. Rev. B* 66, 121404 (2002).
- [15] S. Verlaak, S. Steudel, P. Heremans, D. Janssen, and M. S. Deleuze, *Phys. Rev. B* 68, 195409 (2003).
- [16] K. Ihm, B. Kim, T.-H. Kang, K.-J. Kim, M. H. Joo, T. H. Kim, S. S. Yoon, and S. Chung, *App. Phys. Lett.* 89, 033504 (2006).
- [17] J. Lee, J. H. Kim, and S. Im, *J. App. Phys.* 95, 3733 (2004).
- [18] O. McDonald, A. A. Cafolla, D. Carty, G. Sheerin, and G. Hughes, *Surf. Sci.* 600, 3217 (2006).
- [19] F.-J. M. Heringdorf, M. C. Reuter, and R. M. Tromp, *Nature* 412, 517 (2001).
- [20] M. Alagia, C. Baldacchini, M. G. Betti, F. Bussolotti, V. Caravetta, U. Ekström, C. Mariani, and S. Stranges, *J. Chem. Phys.* 122, 124305 (2005).
- [21] J. Stöhr, *NEXAFS Spectroscopy* (Springer Berlin, Heidelberg, 1992).
- [22] C. Kim, K. Bang, I. An, C. J. Kang, Y. S. Kim, and D. Jeon, *Curr. App. Phys.* 6, 925 (2006).
- [23] T. Yokoyama, K. Seki, I. Morisada, K. Edamatsu, and T. Ohta, *Phys. Scr.* 41, 189 (1990).
- [24] K. Lee and J. Yu, *Surf. Sci.* 589, 8 (2005).
- [25] K. Ihm, S. Chung, T.-H. Kang, and S.-W. Cheong, *App. Phys. Lett.* 93, 141906 (2008).
- [26] C. B. France, P. G. Schroeder, J. C. Forsythe, and B. A. Parkinson, *Langmuir* 19, 1274 (2003).